ADVANCES IN MEASUREMENT AND MODELLING OF BISTATIC SEA CLUTTER

Hugh Griffiths

THALES/Royal Academy of Engineering Chair of RF Sensors
University College London
Gower Street, London WC1E 6BT, UK
h.griffiths@ee.ucl.ac.uk

ABSTRACT

An analysis is presented of the results from recent trials to gather 2.4 GHz bistatic sea clutter, and in particular, of fitting the compound K distribution model both to bistatic clutter data and to simultaneously-acquired monostatic clutter data. It is found that the K distribution provides a good fit to the bistatic data, but that the bistatic clutter is significantly less 'spiky' than that of the equivalent monostatic distribution – i.e. that the tail of the distribution is shorter. This result is important, because it suggests that a bistatic geometry will give improved detection performance of weak targets against a clutter background compared to the conventional monostatic geometry. These results lead to the concept of 'clutter diversity', in which in a multistatic or netted sensor, advantage is taken of a knowledge of the variation of the properties of clutter in this way, as an additional degree of freedom that can be exploited to adaptively optimise the overall radar system performance.

***Index Terms*—** bistatic radar, clutter, radar signal processing

1. INTRODUCTION

Bistatic radar is now regarded as a mainstream subject within the radar domain, as evidenced by the increasing number of publications in journals and at conferences. There are several reasons for this:

- Bistatic radar has potential advantages in detection of targets which are shaped to scatter energy in directions away from the monostatic;
- The receiver is covert and therefore safer in many situations;
- Countermeasures are difficult to deploy against bistatic radar;
- Increasing use of systems based on autonomous air vehicles (UAVs) makes bistatic systems attractive , since bistatic operation may remove the need for a relatively small UAV to carry the heavy, complex and power-hungry transmitter;
- Many of the synchronisation and geolocation problems that were previously very difficult are now readily soluble using GPS, and
- The extra degrees of freedom may make it easier to extract information from bistatic clutter for remote sensing applications.

For these reasons, practical bistatic radar systems are now being built and evaluated. However, if their detection performance is to be understood and optimised it will be necessary to gain a proper understanding of the properties of bistatic radar clutter [1, 2].

The clutter properties of interest are (i) the mean backscatter coefficient σ_B^o, (ii) the amplitude statistics, and (iii) the Doppler spectrum. These will depend not only on all of the parameters associated with monostatic clutter (surface roughness, incidence angle, frequency, polarisation, …) but also on all of the parameters associated with the bistatic geometry. It is perhaps not surprising, therefore, that present knowledge of the properties of bistatic clutter is limited.

The purpose of this paper is therefore to present the results of some recent experimental measurements of bistatic sea clutter, to consider how the results may be used to develop models of bistatic radar clutter, and to point the way to how the results and models might be of use in future sensor systems.

2. THE NETRAD RADAR

The NetRAD system [3, 4] was conceived and built at University College London (UCL) as a three-node coherent multistatic radar test-bed, to be used to make experimental bistatic and multistatic measurements, and to gather data on bistatic radar clutter. It was chosen to operate in the 2.4 GHz licence-exempt Industrial, Scientific and Medical (ISM) band, and was designed to make use of low-cost COTS hardware such that the budget for construction was of order GBP 4,000. In its initial form the transmit power at each node was 200 mW, giving a maximum range against small targets of order 2 km.

Control and synchronisation of the nodes was achieved by physical cable connection, up to a maximum node separation of 50 m, but as the NetRAD system evolved, the wired communication links that were used for control and synchronisation between the radar nodes became a limitation. While these wired links had initially been the most effective link options in terms of cost and simplicity, to extend the distance between the radar nodes in the array to several kilometres by this means was unfeasible. This led to a requirement for both wireless communications, and wireless carrier synchronisation and triggering.

The Global Positioning System Disciplined Oscillator (GPSDO) was identified as a suitable means to provide the required carrier synchronisation, utilising long-term stable, ovenised Quartz oscillators which are corrected with reference to the 1 Hz GPS time mark which is actively steered towards UTC time.

GPS time transfer provides a long-term stable time standard which is traceable to that of a Rubidium atomic source. It is very convenient since it is available for free, almost everywhere on Earth, whenever there is a clear view of the sky. It can be utilized using cheap and readily available receivers. Multistatic carrier synchronisation can be performed autonomously, without the requirement of line-of-sight or cable medium, and across vast baselines. However, the long-term stable GPS time mark exhibits a large amount of short term phase jitter. This phase jitter can be removed by phase-locking to a high quality oscillator.

The University of Cape Town (UCT) has designed and built three GPSDOs [5] to evaluate the possibility of multistatic radar synchronization, and these have been integrated with the UCL NetRAD radar. The UCT GPSDOs are unique in that they are designed as research platforms that provide full access and control to all significant parameters via two serial ports.

A further upgrade was to increase the transmit power at one node to 500 W, giving greater sensitivity and longer range. Table 1 lists the principal system parameters, and Figures 1, 2 and 3 show the radar hardware deployed.

TABLE I
PRINCIPAL NETRAD SYSTEM PARAMETERS

frequency	2.4 GHz
bandwidth	50 MHz
nominal range resolution	3 m
PRF	50 Hz – 3 kHz
pulse length	0.1 – 10 μs
waveforms	digitally-generated: linear FM chirp, Barker codes, polyphase codes, etc
transmit power	500 W
antenna gain	23 dBi
antenna beamwidth	10º × 10º

Fig. 1. NetRAD hardware for one node deployed in a truck.

Fig. 2. Close-up of NetRAD radar antenna. The azimuth/elevation mount allows a pointing precision of better than ±1º. The beamwidth in both planes is approximately 10º.

Fig. 3. NetRAD transmit/receive node, showing separate radar transmit and receive antennas, and GPS and wireless link antennas.

3. TRIALS

Proving trials were undertaken at Peacehaven, Sussex, on the south coast of England during July and August 2010, to assess the operation of the system before shipping the radar to South Africa. Trials in South Africa were undertaken in the Western Cape area near Simon's Town in October 2010, and included measurements of bistatic sea clutter at low grazing angle, in-plane bistatic sea clutter measurements at higher grazing angle, and bistatic measurements of co-operative small maritime targets and their wakes.

3.1. First measurements of bistatic sea clutter [6]

First measurements of sea clutter were made at Peacehaven with two nodes (transmitter/receiver and receiver) separated by a baseline of 96 m and located on a clifftop at a height of 60 m above sea level. The bistatic angle and grazing angle were therefore a function of range; the bistatic angle (β) varied from 18º at short range to 8º at long range, and the grazing angle (ψ_g) varied from 12º at short range to 5º at long range. Figure 4 shows the geometry. The antenna positions were fixed and the change in the bistatic angle was achieved by range gating the data.

The wind speed was approximately 25 knots (13 ms^{-1}) from the south-west, and the swell direction was towards the shore.

The data was fitted to the K+noise distribution [7, 8], whose pdf in terms of intensity can be written as:

$$P_{C+N}(I) = \int_0^\infty \frac{b^{\nu}x^{\nu-1}}{\Gamma(\nu)}\frac{\exp(-bx)}{x+p_n}\exp\left(\frac{-I}{x+p_n}\right)dx \qquad (1)$$

where I is the intensity, x is the local clutter power, ν is the shape parameter, p_n is the noise power, $b = \nu/\sigma_{BW}$ is the scale parameter and σ_{BW} is the average clutter power. The clutter to noise ratio is given by CNR = σ_{BW}/p_n. When the CNR was greater than 30 dB the effect of noise was ignored.

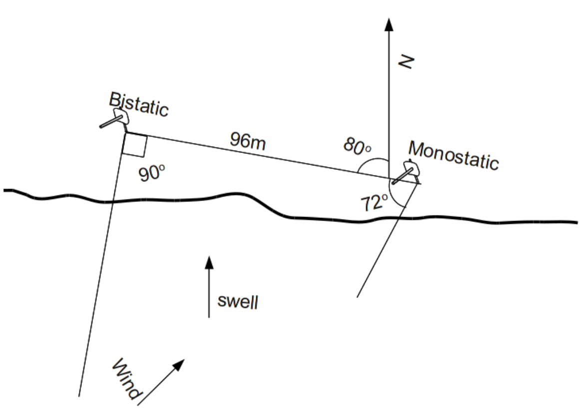

Fig. 4 Geometry for the proving trials at Peacehaven.

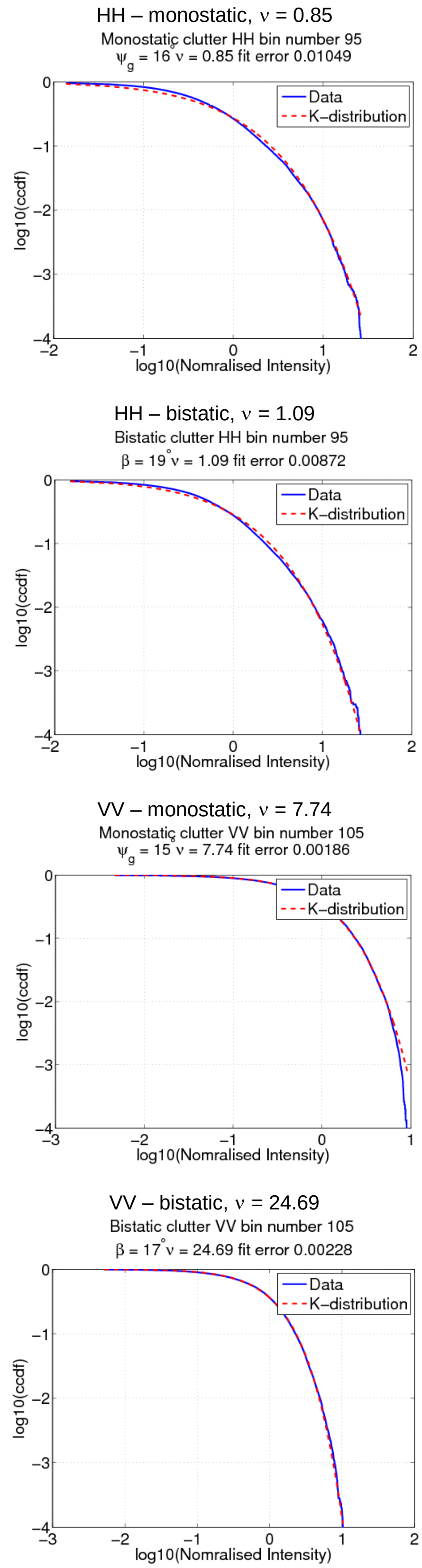

Fig. 5 Fits of the compound K-distribution model to monostatic and bistatic HH and VV polarisation sea clutter data.

The fitting was performed using a Fibonacci search algorithm [9] to find the best fit shape parameter, minimising the rms error between the complementary cumulative distribution function (ccdf) of the data and the numerically generated K+noise data. Moment matching was used to provide the initial value to the algorithm. The ccdf is given by:

$$\Pr\left(I > I_T\right) = \int_{I_T}^{\infty} P_{C+N}\left(I\right) dI \qquad (2)$$

where I_T is the detection threshold. Equation (2) was evaluated numerically using the code from Radar Works [10].

Figure 5 shows examples of the fits. It can be seen that the K distribution+noise fits provide a good representation of the experimental data. In particular, for both HH and VV polarisation the value of the shape parameter ν is greater for the bistatic clutter than for the monostatic (1.09 compared to 0.85 for HH polarisation; 24.69 compared to 7.74 for VV polarisation). When comparing bistatic and monostatic returns data from the same range bins were used. In almost all cases the shape parameter ν was larger for the bistatic channel than for the monostatic channel. In all cases the values of shape parameter were much smaller at HH polarisation than for VV.

3.2. Further measurements of bistatic sea clutter [11]

Of the trials undertaken in South Africa, results are reported here from measurements made on 5 October 2010 on the west side of the Cape of Good Hope, at vertical polarisation. The geometry is shown in Figure 6.

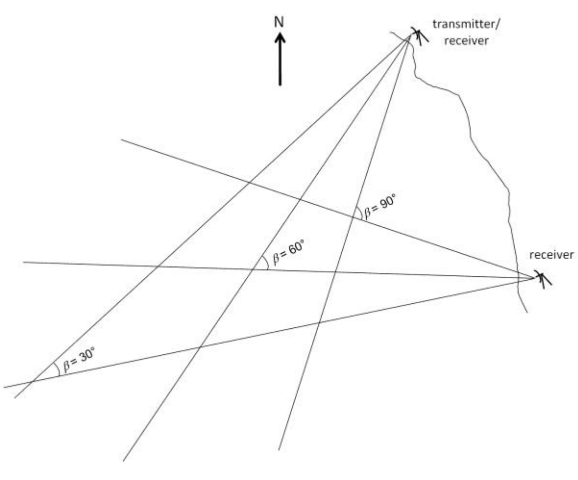

Fig. 6. Geometry for the bistatic measurements. The baseline separation between nodes was 416 m; the orientation of the baseline was 330º with respect to True North. The monostatic ranges corresponding to each bistatic angle are listed in the first column of Table 2.

TABLE III
SUMMARY OF RESULTS. THE SUBSCRIPTS M AND B REFER TO MONOSTATIC AND BISTATIC RESPECTIVELY.

R_M m	β	σ^o_M dB m^2/m^2	σ^o_B dB m^2/m^2	CNR_M dB	CNR_B dB	ν_M	ν_B
805	30º	−59.2	−58.7	18.1	21.5	0.93	3.11
417	60º	−47.1	−47.6	36.9	40.2	0.22	0.48
295	90º	−44.1	−55.8	41.1	35.6	0.17	1.04

The differences in clutter-to-noise ratio (CNR) are due to the higher noise figure in the monostatic receiver caused by the Transmit/Receive (T/R) switch and the larger cell area in the bistatic configuration. The results in Table 2 show that there was no significant difference between monostatic and bistatic reflectivities with changing bistatic geometry, except at a bistatic angle of 90 degrees. This lack of variation of backscatter coefficient with bistatic angle is not typical of bistatic clutter data reported in the literature, as described in [1]. However there are some similar results reported in [12] for vertically polarized, low sea state returns.

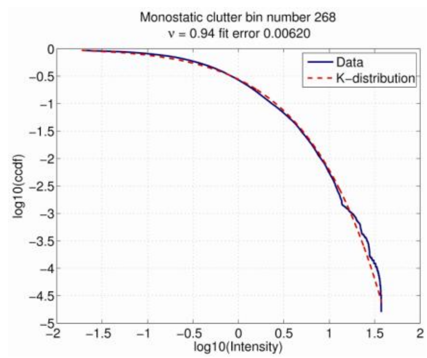

Fig.7. Fit of K+noise model to measured monostatic clutter. Horizontal axis is the log of the intensity normalized to mean; vertical axis is the log of the complementary cumulative distribution function.

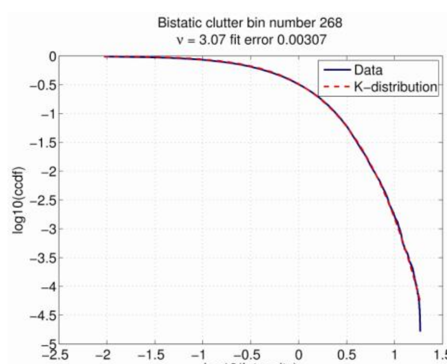

Fig.8. Fit of K+noise model to bistatic clutter measured simultaneously to that of Fig.7. Horizontal axis is the log of the intensity normalized to mean; vertical axis is the log of the complementary cumulative distribution function.

It can be seen that the fit, as measured by the rms error, is good in both cases, but better for the bistatic data. In all cases in Table 2 the value of the shape parameter for the bistatic clutter ν_B is greater than that for monostatic clutter ν_M, showing that the bistatic clutter is less ‘spiky’, in the same way as for the results in section 3.1. The fact that the same effect has been observed consistently, at two different locations, geometries and sea states, suggests that the result may be general, but significantly more work needs to be done to verify this.

The significance of these results is that they suggest that a bistatic geometry will allow a lower detection threshold for a given probability of false alarm, and hence give improved detection performance of weak targets against a clutter background compared to the conventional monostatic geometry. In practice this improvement is not straightforward to evaluate, because as well as the change in clutter statistics from monostatic to bistatic geometry, possible changes in target RCS and in mean clutter RCS should also be taken into account.

It is also worth remarking that a similar effect has been observed in analysing the statistics of bistatic SAR images of urban land target scenes [13]. In that case it is easy to see that the scattering from dihedrals formed by building walls and the ground would result in strong monostatic scattering, but not bistatic, and hence that the monostatic clutter would be spikier. The same effect might be expected of vegetation, in which dihedrals are formed by vertical stalks or trunks and the ground. However, in the case of scattering from the sea surface the physical mechanism that might account for the observed effects is less easy to understand, and indeed, these results may provide some insight that may

4. CLUTTER DIVERSITY

These results lead to the concept of *clutter diversity*. Essentially, the foregoing results have shown that in a multistatic or networked radar, the properties of clutter depend on the bistatic geometry, and that some geometries yield more favourable detection performance than others. Clutter Diversity is a matter of understanding these variations and their dependencies, and hence providing an additional degree of freedom that can be exploited to adaptively optimise the overall radar system performance.

Clutter diversity may therefore take its place alongside waveform diversity, spatial diversity, code diversity, polarisation diversity and others, as a domain in which radar performance can be optimised.

5. TARGET BISTATIC SIGNATURE MEASUREMENTS

Finally, as well as the measurements of clutter characteristics, measurements were also made of the signatures of small maritime targets and their wakes. An example is shown in Figure 9 of a Rigid Hull Inflatable Boat (RHIB) performing circling manoeuvres over a period of about two minutes. The first and second plots show range (horizontally) versus time (vertically), and range (horizontally) versus Doppler (vertically), and show the expected periodic variation of range and Doppler.

The third plot shows Doppler (vertically) versus time (horizontally), and some interesting detail is evident. It appears that as well as the signature of the RHIB itself, there is a component with higher peak Doppler shift which may correspond to a bow wave, and an intermittent, stronger component at zero Doppler which may be due to spray. There is certainly more to be done to understand these signatures and their variation with bistatic geometry.

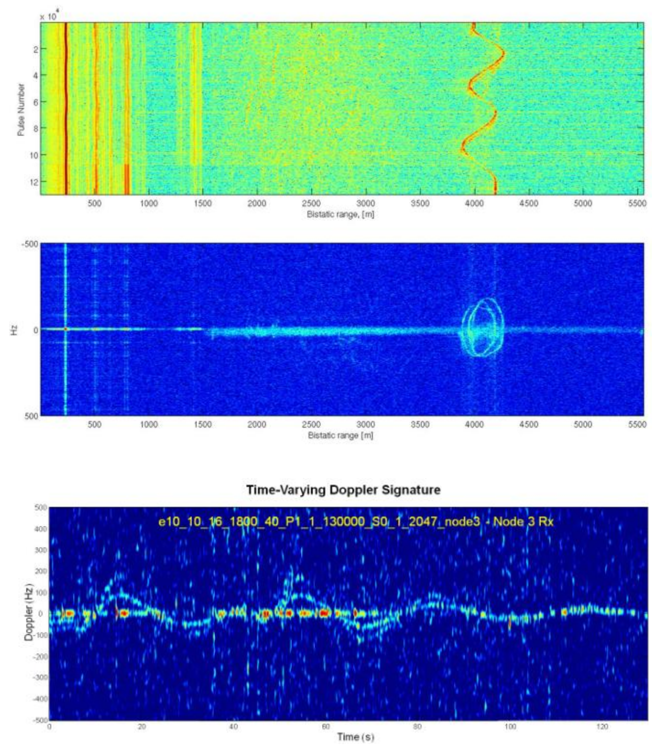

Fig. 9. Measured bistatic signature of a RHIB target performing circling manoeuvres, over a period of about two minutes. The lowermost plot was produced by Dr Victor Chen.

6. SUMMARY AND CONCLUSIONS

This paper has reported and analysed some recent measurements of bistatic radar sea clutter. The NetRAD radar sensor represents a unique and versatile instrument, and the data have yielded some interesting and potentially significant results.

Analysis of the amplitude statistics of bistatic sea clutter and comparison with simultaneously-measured monostatic clutter has shown firstly that the compound K-distribution model provides a good fit to the measured data. Secondly, in the examples analysed to date it has been found that the bistatic clutter distribution is shorter-tailed than the equivalent monostatic clutter, which suggests that a bistatic geometry will allow a lower detection threshold for a given probability of false alarm, and hence give improved detection performance of weak targets against a clutter background.

This has led to the introduction of the term 'clutter diversity': the work has shown that in a multistatic or networked radar the properties of clutter depend on the bistatic geometry, and some geometries yield more favourable detection performance than others. Clutter Diversity is a matter of understanding these variations and their dependencies, and hence providing an additional degree of freedom that can be exploited to adaptively optimise the overall radar system performance.

Further experiments with this radar are planned, as well as extension to multi-band operation and the provision of an array receiver which will allow bistatic SAR and bistatic STAP operation.

7. ACKNOWLEDGEMENTS

I express my thanks to all of the people who have contributed to the development of the NetRAD radar and the conduct of the trials and analysis of results, and to ONR (Global), THALES UK, THALES Nederland, the Engineering and Physical Sciences Research Council and the Royal Academy of Engineering for their financial support for this work.

8. REFERENCES

[1] H.D. Griffiths, W.A. Al-Ashwal, K.D. Ward, R.J.A. Tough, C.J. Baker and K. Woodbridge, 'Measurement and modelling of bistatic radar sea clutter', *IET Radar Sonar and Navigation*, Vol.4, No.2, pp280-292, March 2010.

[2] N.J. Willis and H.D. Griffiths (eds), *Advances in Bistatic Radar*, SciTech Publishing Inc., Raleigh, NC, ISBN 1891121480, 2007.

[3] T.E. Derham, K. Woodbridge, C.J. Baker and H.D. Griffiths, 'The design and development of an experimental netted radar system', International Conference *RADAR 2003*, Adelaide, Australia, pp. 293–298, September 2003.

[4] T.E. Derham, S. Doughty, K. Woodbridge and C.J. Baker, Design and evaluation of a low-cost multistatic netted radar system, *IET Radar Sonar and Navigation*, Vol.1, No.5, pp362–368, October 2007.

[5] M.R. Inggs, H.D. Griffiths, K. Woodbridge, W.A. Al-Ashwal, J.S. Sandenbergh and G.E. Inggs, 'Experimental coherent networked radar using GPS-disciplined reference oscillators', *Cognitive Systems with Interactive Sensors*, Crawley, 22 November 2010.

[6] W.A. Al-Ashwal, C.J. Baker, A. Balleri, H.D. Griffiths, R. Harmanny, M. Inggs, W.J. Miceli, M. Ritchie, J.S. Sandenbergh, A. Stove, R.J.A. Tough, K.D. Ward, S. Watts and K. Woodbridge, 'Measurements of bistatic radar sea clutter', *IEEE Radar Conference 2011*, Kansas City, MO, 23–27 May 2011.

[7] K.D. Ward, R.J.A. Tough and S. Watts, *Sea Clutter: Scattering, the K-Distribution and Radar Performance*, IET, London, 2006.

[8] S. Watts, 'Radar detection prediction for targets in both K-distributed sea clutter and thermal noise', *IEEE Trans. Aerospace and Electronic Systems*, vol.AES-23, No.2, pp40-45, January 1987.

[9] R. Bronson, *Schaum's Outline Series Theory and problems of Operations Research*, McGraw-Hill, 1982

[10] G. Davidson, 'Radar Works', http://www.radarworks.com/, Accessed Jan. 2011.

[11] W.A. Al-Ashwal, C.J. Baker, A. Balleri, H.D. Griffiths, R. Harmanny, M. Inggs, W.J. Miceli, M, Ritchie, J.S. Sandenbergh, A. Stove, R.J.A. Tough, K.D. Ward, S. Watts and K. Woodbridge, 'Statistical analysis of simultaneous monostatic and bistatic sea clutter at low grazing angles' *Electronics Letters*, Vol.47, No.10, pp621–622, 12 May 2011.

[12] G. Ewell and S. Zehner, 'Bistatic sea clutter return near grazing incidence', *Proc. IEE International Conference RADAR 82*, IEE Conf. Publ. No. 216, pp188–192, October 1982.

[13] G.A. Yates, 'Bistatic Synthetic Aperture Radar', PhD thesis, University College London, January 2005.